

Article

Load-Carrying Capacity of Bailey Bridge in Civil Applications

Jozef Prokop ^{1,*}, Jaroslav Odrobiňák ¹, Matúš Farbák ¹ and Vladimír Novotný ²

¹ Department of Structures and Bridges, Faculty of Civil Engineering, University of Žilina, Univerzitná 8215/1, 010 26 Žilina, Slovakia; jaroslav.odrobinak@uniza.sk (J.O.); matus.farbak@uniza.sk (M.F.)

² Tebrico Ltd., P.O. Hviezdoslava 8, 010 01 Žilina, Slovakia; tebrico@tebrico.sk

* Correspondence: jozef.prokop@uniza.sk

Abstract: The paper presents an extensive study aimed to determine the applicability of the demountable Bailey bridge (BB) system on construction sites or in other temporary conditions while meeting the regulations for the design and assessment of steel bridges. The analysis is focused on whether and to what extent the BB system with spans between 12 and 36 m is usable for on-site freight transport with conventional lorries with a total weight of up to 22–28 tons. At the same time, the BB system within these spans should be utilized for construction vehicles with a total weight of up to 32–40 tons. To calculate the load-carrying capacity, spatial numerical models were analysed using FEM and procedures of actual design codes were utilized. In the case of the main girders, analysis is focused on the out-of-plane stability of their compressed chords. Recommendations for the use of this bridge system in different arrangements of the main girder and bridge deck are then summarized and discussed.

Keywords: Bailey bridge; load-carrying capacity; stability; steel bridge; temporary bridge



Citation: Prokop, J.; Odrobiňák, J.;

Farbák, M.; Novotný, V.

Load-Carrying Capacity of Bailey Bridge in Civil Applications. *Appl. Sci.* **2022**, *12*, 3788. <https://doi.org/10.3390/app12083788>

Academic Editors: Algirdas Juozapaitis and Alfonsas Daniūnas

Received: 1 March 2022

Accepted: 5 April 2022

Published: 8 April 2022

Publisher's Note: MDPI stays neutral with regard to jurisdictional claims in published maps and institutional affiliations.



Copyright: © 2022 by the authors. Licensee MDPI, Basel, Switzerland. This article is an open access article distributed under the terms and conditions of the Creative Commons Attribution (CC BY) license (<https://creativecommons.org/licenses/by/4.0/>).

1. Introduction

Temporary bridge structures were mainly developed for military purposes in the past. Very often, they also served to ensure rapid access through rural unexplored areas [1,2]. Increasingly, originally military emergency ones are also used for civil purposes (Figure 1), where their adaptability, low weight, but especially extremely fast erection and almost immediate usability for traffic are utilized.



Figure 1. Bailey bridge (TS-12 + TD-33) over Vah river during construction (Slovakia).

Currently, a significant number of these structures are used when natural disasters destroy a part of transport infrastructure. Their application as temporary bridges on

larger construction sites is also growing (Figure 2). In addition, they are used as ‘short-term’ temporary (semi-permanent) bridges on local and rural or unpaved roads when the construction of a permanent bridge is still financially inefficient or not possible due to traffic issues (Figure 3).



Figure 2. Bailey bridge (TD-36 + 36) placed on construction site road over Orava river (Slovakia).



Figure 3. ‘Long-term’ temporary bridge Bailey bridge (DS-15 + 21 + 27 + 21) over Lužnice river (Czech Republic).

One of the more popular systems of this category is the Bailey bridge system [3]. The Bailey bridge (BB) was invented by Donald Bailey as a military bridge about 80 years ago [4]. After the first decade, it was proven to be an innovative and successful bridge system that can be built efficiently and quickly [5]. Additionally, this temporary bridge system is currently used in many countries for civil purposes as mentioned above. However, the maximum load-carrying capacity for such a use is not commonly available. For instance, static verification is usually demanded for every application in civil conditions in Slovakia. In the case of longer term use, and in situ load test is also required [6].

Nowadays, loads according to [7] are applied for military purposes. However, the aim of the presented study is to point out the actual possibilities of this very old structural temporary bridge system in some civil applications. Therefore, the paper presents a study on whether and to what extent the BB system with spans between 12 and 36 m is usable for transport considering conventional lorries with a total weight up to 22–28 tons. At the same time, isolated construction vehicles with a total weight up to 32–40 tons can also be allowed to pass the bridge.

2. Outline of the Study

For the purposes of the analysis, the load-carrying capacity of individual bridge members was selected as a decisive criterion for the applicability of the BB system. Based on experience, double-truss and triple-truss main girders were taken into account as single-story and double-story alternatives:

- Double-truss, single-story (DS) for a span with length of 12.196 m;
- Triple-truss, single-story (TS) for spans: 12.192 m, 15.240 m, 18.288 m and 21.336 m;
- Double-truss, double-story (DD) for spans: 21.336 m, 24.384 m and 27.432 m;
- Triple-truss, double-story (TD) for spans: 27.432 m, 30.480 m, 33.528 m, and 36.576 m.

In Table 1, the seven chosen variants are presented, which were identified as most suitable and applicable after evaluating several alternatives.

Table 1. Spans and BB arrangement of the chosen alternatives.

Span	Truss	Story	Abbreviation
40 ft/12.192 m	triple	single	TS-12
60 ft/18.288 m	triple	single	TS-18
70 ft/21.336 m	triple	single	TS-21
80 ft/24.384 m	double	double	DD-24
90 ft/27.432 m	double	double	DD-27
110 ft/33.528 m	triple	double	TD-33
120 ft/36.576 m	triple	double	TD-36

All bridges are supposed to act as simply supported, while the end verticals of BB are present on both ends of main girders. It is further assumed that standardized bearings of the BB system are used to transfer reactions from the superstructures to substructures.

With respect to the structural arrangement of the BB system [3], the load-carrying capacities were derived from the resistance of following members or their cross-sections (the terminology of Bailey bridge from [3] is given in single quotation marks, if differ from the common bridge engineering terminology):

- Stringers (Figure 4)
 - Old stringers made of the original cross-section.
 - New stringers made of the cross-section IPN100.
 - Alternative new stringers made of the cross-section IPN120.
- Cross beams—‘transoms’.
- Panel of truss girders.
 - Upper chord.
 - Bottom chord.
 - Diagonals with U-shaped cross-section.
 - Alternative diagonals with I-shaped cross-section.
 - Verticals with U-shaped cross-section.
 - Alternative verticals with I-shaped cross-section.
- End verticals—‘end posts’.
- Inclined struts—‘rakers’.
- Panel pin (hinged connection between panels).
- Bottom bracings—‘sway brace’.
- Floor bolts (in double-storeys arrangement)—‘chord bolts’.

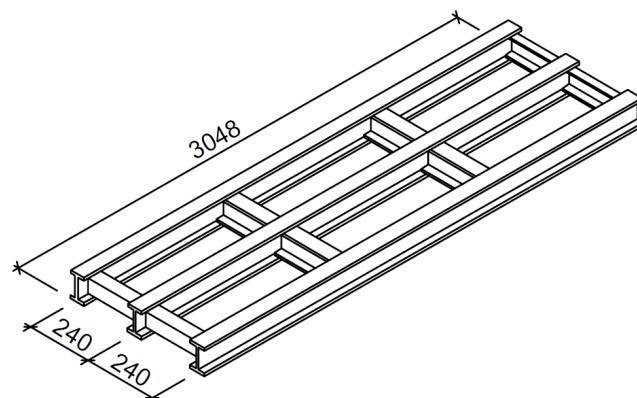


Figure 4. Scheme of three-stringer panel.

The load-carrying capacity of the bridge deck was determined for two variants of the construction arrangement of cross beams according to Figure 5:

- Three cross beams within each panel of the bridge—the spans of the stringers are then 1440 + 1290 + 318 mm.
- Two cross beams within each panel of the bridge—the spans of the stringers are then 1608 + 1440 mm (this alternative was applicable only for single-story systems).

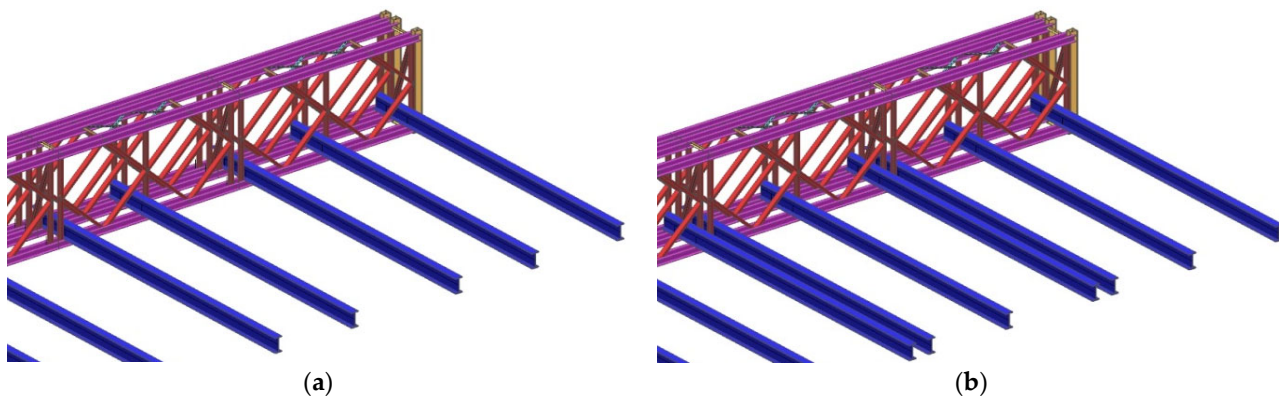


Figure 5. Two alternatives of construction arrangement of cross beams: (a) 3 cross beams within each panel; and (b) 2 cross beams within each panel.

The variant with four cross beams within each panel was not considered in the study.

In addition, two alternatives to the timber roadway deck cover solution given in Figure 6 were considered:

- Standard solution of two layers of 2 × 50 mm thick timber boards, where the bottom boards are placed perpendicular to the stringers, while the top layer is oriented in 45° degrees to the bridge axis;
- Stiffer roadway, where bottom supporting layer of the bridge deck is made of timber beams of 100 mm section height placed side by side perpendicular to the stringers, while the top layer stays the same as in the alternative a).

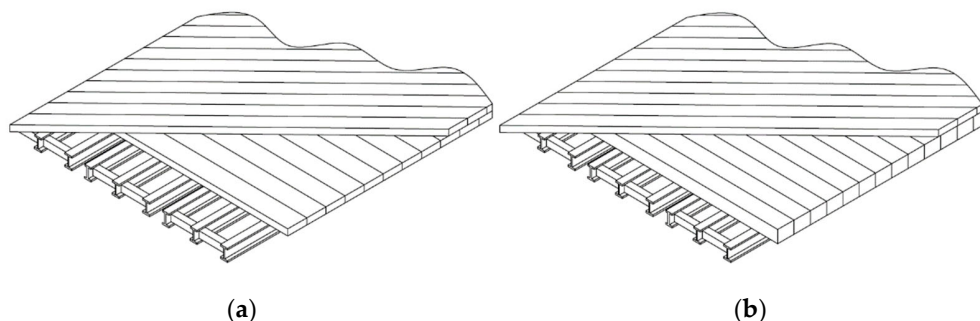


Figure 6. Two alternatives of timber roadway deck: (a) standard solution of timber deck; and (b) more stiff timber deck.

3. Global Analyses

3.1. Numerical Models

Several studies have been executed to verify the static and dynamic behaviour of Bailey bridge structures by in situ loading tests and numerical analyses [8–10].

The global analyses of all alternatives of the BB in the present study were carried out using spatial computational FEM models properly derived in the commercial software SCIA Engineer [11]. This software was selected as it is commonly used in design practice for bridge structures. The application of a more complex approach was not considered since it is believed that it would increase the computational effort without significantly improving the quality of the results [12,13].

Beam-type elements, with six degrees of freedom at each node were applied for the steel members of the BB superstructure, Figure 7. The one-dimensional elements are confirmed to be suitable for approximation of such type of structure [14,15]. The geometry and individual dimensions of steel elements fully respect the BB bridge layout [4,5]. It was assumed that each alternative of the bridge is completely assembled. All relevant geometrical and cross-sectional characteristics were taken into account. Each connection of cross beams to the bottom chords of panels was performed considering a semi-rigid joint connection with a stiffness of 150 MN/m in compression and with stiffness of 60 MN/m in tension, but with zero rotational stiffness in all directions, so that approximates the real behaviour of perfectly tightened ‘transom clamp’. The eccentric junctions of continuous stringers and cross beams can be modelled as hinged while allowing for their certain longitudinal displacement over the cross beams. The sway brace elements were modelled as rods capable of bearing tension forces only. Based on non-destructive hardness tests on actual bridges of this type, steel with yield strength $f_y = 360$ MPa was considered for the needs of the presented study. Modulus of elasticity $E = 210,000$ MPa was utilized in the analysis as well.

The timber deck does not interact with other bearing components due to negligible stiffness of its connection to the stringers. The only function of the timber deck is to provide the carrying surface for passing vehicles. Therefore, the timber deck of the bridge was introduced into the model by shell elements with reduced modulus of elasticity to a very small value [$E_{deck} = 10$ MPa]. This almost completely prevented the interaction of the deck with the steel elements of the bridge deck, but it made it possible to place a traffic load anywhere on the surface of the bridge deck. The second advantage of this modelling approach is that it allows the redistribution of a modelled traffic load to the corresponding stringers. Figures 8 and 9 present the finished models for the shortest and the longest span analysed in the study.

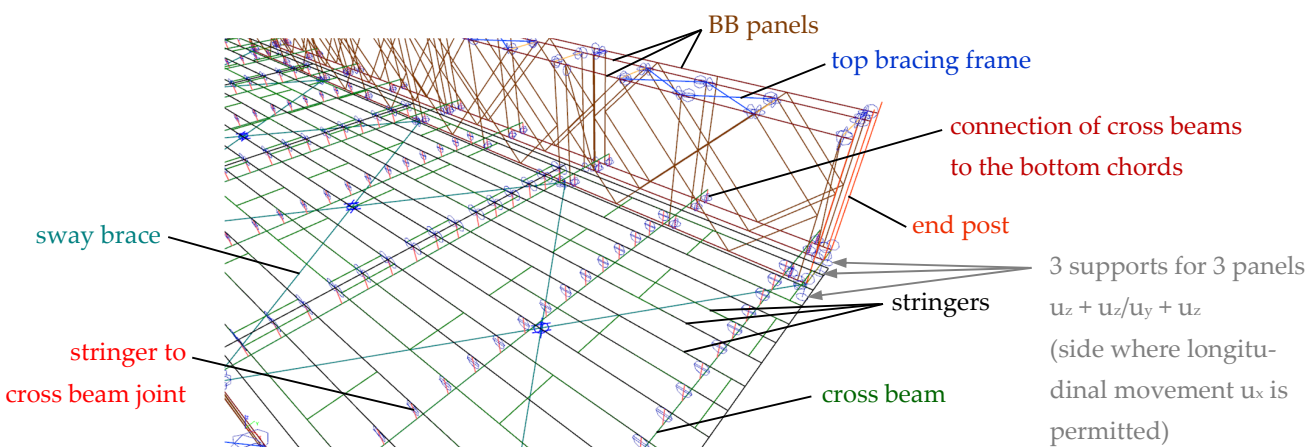


Figure 7. Some notes on spatial FEM models of steel superstructure of Bailey bridge.

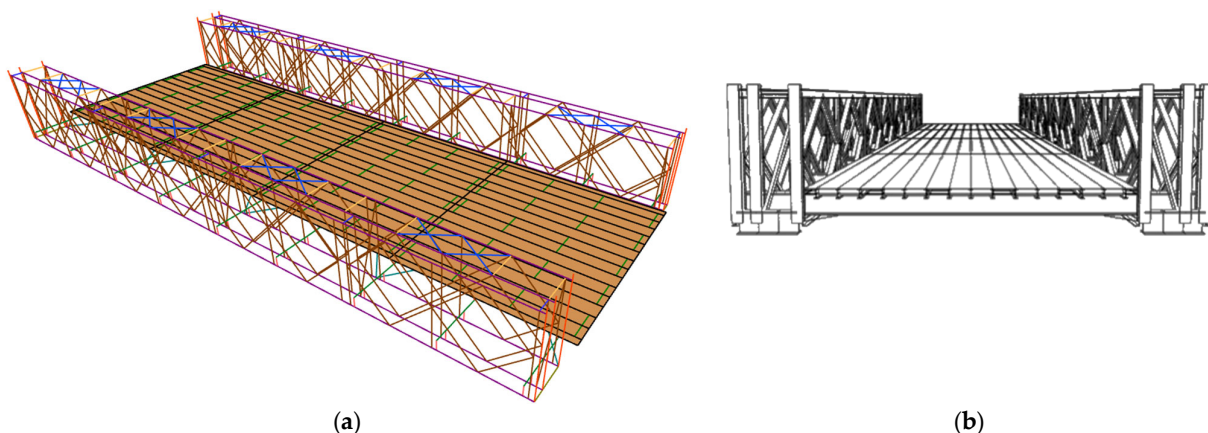


Figure 8. Geometry of complete spatial FEM model in the case of the shortest analysed span TS-12 (40 ft): (a) model from beam and shell elements; and (b) front view visualization.

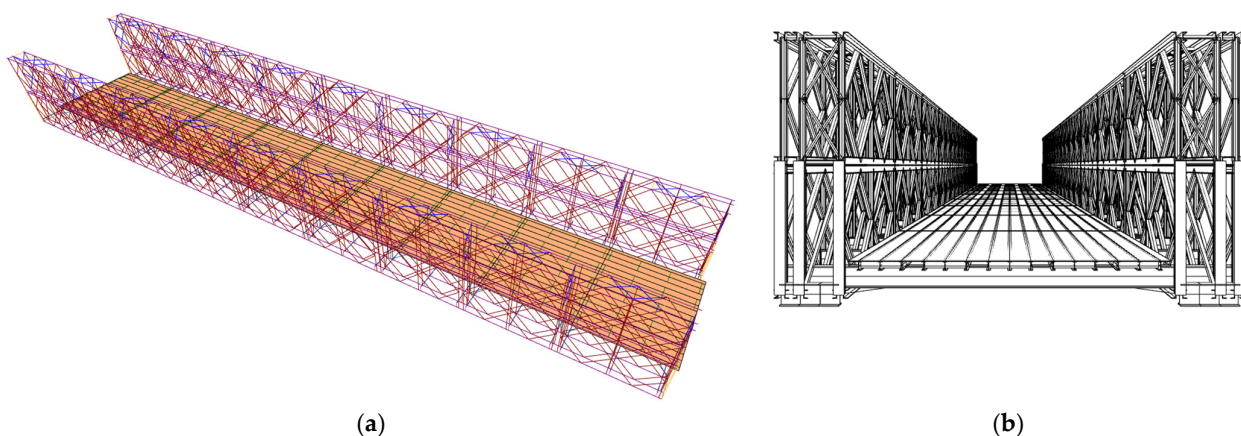


Figure 9. Geometry of compete spatial FEM model in the case of the longest analysed span TD-36 (120 ft): (a) model from beam and shell elements; and (b) front view visualization.

Linear elastic static analysis was performed to obtain the results. Due to the type of the structure, both 2nd order effects and imperfections were implemented into the evaluation process indirectly by so-called ‘equivalent column method’, where individual stability checks using appropriate buckling lengths corresponding to the global buckling mode of the structure were utilized [16].

3.2. Loads in Global Analysis

In addition to the respective dead load corresponding to the layout of the superstructure and bridge deck, traffic loads and wind effects were taken into account.

Within the scope of this study, wind loads were considered as F_w^* according to Eurocode 1 [17] and were properly combined with the traffic loads. Accordingly, the wind pressure value of $q_{p,z} = 0.50 \text{ kPa}$ was considered acting uniformly for all analysed BB models. The effect of wind pressure acting on bridge deck combined with pressure on traffic load was transformed into the edge horizontal load, surface horizontal load and vertical surface load producing torsion of the deck around its longitudinal axis, as shown in Figure 10a. The values presented in Figure 10a were derived by utilizing the reference height of traffic load 2.0 m consistent with [17]. Accordingly, the wind load on structural members of BB panels was calculated as uniformly distributed load using the force coefficient c_f given in [17] with dependence on the shape of each cross-section, as shown in Figure 10b.

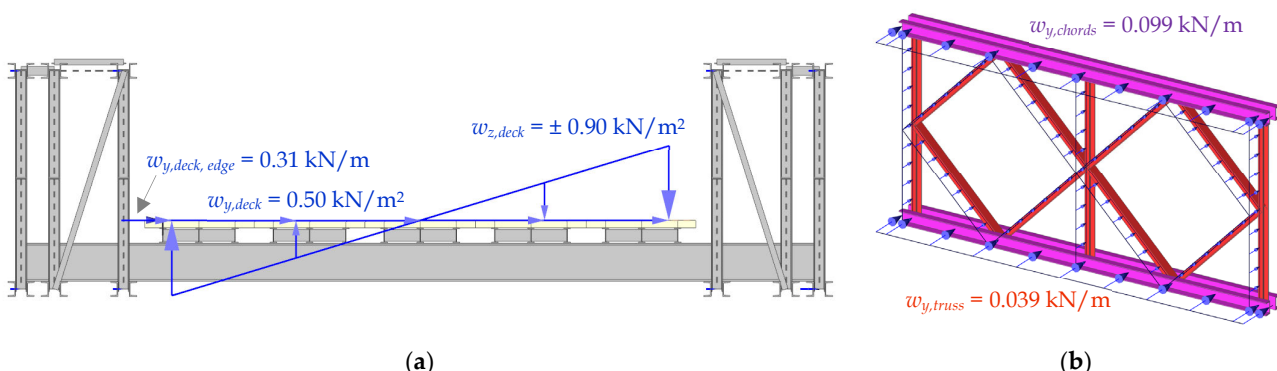


Figure 10. Example view from approximation of wind load: (a) left wind action on deck with traffic load on it; and (b) wind load assumed on main girders BB panels.

Due to its variable nature, modelling of traffic loads presents the key input in the assessment of both the new bridges and, of course, existing ones. Load models defined in the current design codes are often described as conservative, due to the limited traffic data used for their calibration and their integrated safety levels [18]. In addition, despite the harmonized design codes for almost all European countries, the structural safety levels and consequent capacities of similar bridges vary across Europe, as different national adjustment factors are defined in most of countries. Code load schemes are primarily developed for new-designed bridges expecting to be in service next hundred years, at least. Nowadays, extensive research is aiming to find out the ‘actual tonnage’ which can occur on the bridge without any traffic restrictions. Thus, for the load schemes representing the traffic load in the present study, it was decided not to use the load schemes given in Eurocode 1 [19]. The main reasons for avoiding the Eurocode statements for ‘normal’ traffic in the case of the Bailey bridges arose from the fact that it is still difficult to define which part of the LM1 scheme according to [19] can be considered as a representative vehicle. This problem is also evident from the experiences from recalculations of old bridges, supported by the extensive theoretical study presented in [20,21]. Specifically, in [20], some results from the extensive study are published, based on several thousands of calculated bending moments and shear forces for bridges with different concepts of cross-sections and spans. In the follow-up research presented in [21], over 2800 load-carrying capacities for those bridges were quantified and compared, considering different load schemes, including possible alternatives from the Eurocode models [19]. In addition, different calculations of the current load capacity of the bridges were taken into account in those calculations, thus considering their possible poor condition. The final value of load-carrying capacity produced by representative loads depend also on mutual combinations of classification factors α_{Qi} and α_{qi} [19]. Moreover, in the case of short spans, LM1 causes disproportionately high effects because the dominant ‘uniformly distributed load’ (UDL)

as well as the dominant ‘tandem system’ (TS) are concentrated together in the same lane on the relatively small length section. The abovementioned phenomenon is even more visible in narrow bridges. Findings that the load schemes given in the Eurocode [19] are not very suitable for load-carrying capacity calculations of existing bridges are also supported by the conclusions in [22], which provides an extensive state of the art presentation of the traffic load models.

Thus, the schemes shown in Figures 11 and 12 were taken into account. These schemes come from the former Slovak national code and were slightly modified for the purpose of narrow bridges. These load schemes, utilized for several decades, reflect more to the traffic situations in narrow bridges [21], especially, when the load-carrying capacity of the bridge will be probably limited by the elements of member steel deck. Another advantage is that the required vehicle weight, which represents the instantaneous permissible weight of vehicle passing the bridge, is relatively clearly defined therein [20,21].

Thus, the load scheme in Figure 11 is a better approximation for the possible traffic situation on such a narrow temporary bridge, with one of the lorries being considered as the *normal load-carrying capacity* V_n . The ‘normal load-carrying capacity’ represents the maximum permissible weight of any vehicle on the bridge without any restrictions or addition regulations in traffic within the road section on the bridge. Geometric parameters of the load scheme are presented in Figure 11.

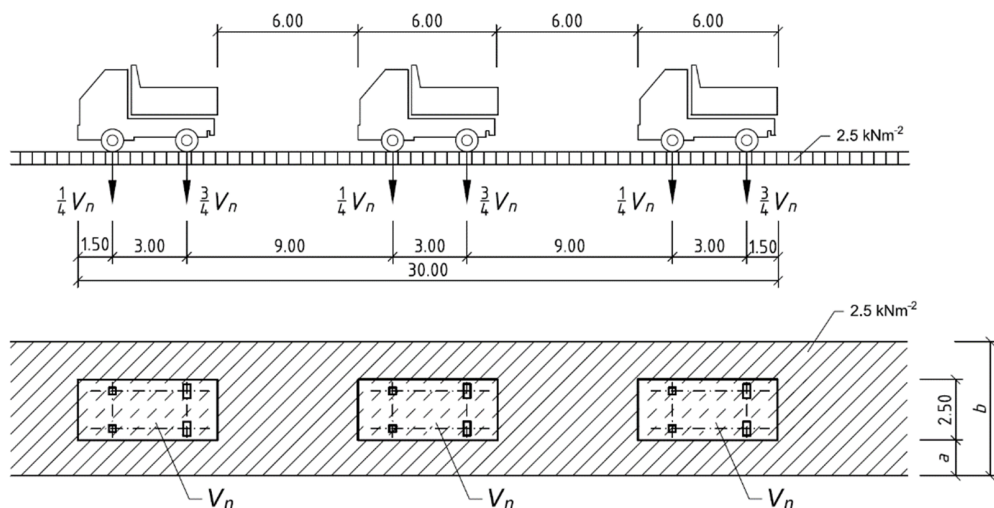


Figure 11. Load scheme used for normal load-carrying capacity.

The *exclusive load-carrying capacity* V_e represents maximum permissible weight of a single lorry on the bridge, while no other vehicles on the bridge are allowed at the same time, e.g., by other traffic signs. In the case of analysed Bailey bridges, which are the narrow one-lane bridges, this can be easily specified by the traffic sign of minimum following distance between vehicles. Alternatively, in some countries, the additional text table to normal load carrying capacities sign can be installed where the text concerning the maximum weight of the only vehicle on the bridge is specified.

In the present study, for the ‘exclusive’ load scheme, it was decided for practical reasons to use the heavy truck scheme shown in Figure 12 instead of the schemes given in [19], which again differ among countries. To cover all the alternatives in that table, fourteen different trucks should be evaluated. Thus, the adopted scheme from Figure 12 is able to produce more efficient load effect with the simpler load-modelling, as only the distance of middle axes d has been changing from 4.0 m to the most severe alternative 1.20 m. That means that the vehicle should be the only traffic load on the bridge as discussed previously.

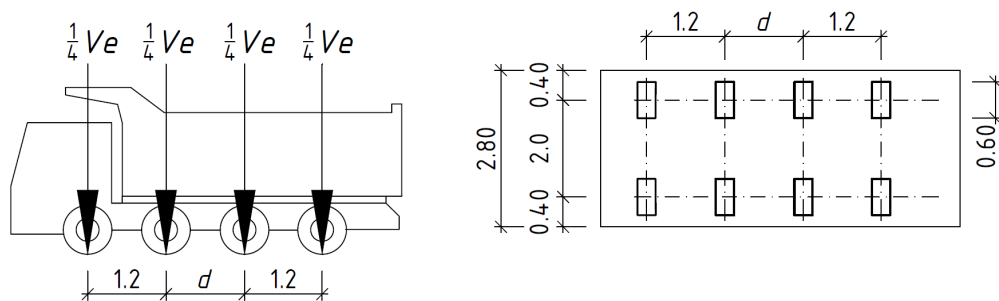


Figure 12. Scheme of vehicle used for exclusive load-carrying capacity.

Heavy vehicles from the schemes given in Figures 11 and 12 could be placed in any position within the cross-section of free width 3.30 m between timber curbs, as can be seen in Figure 13.

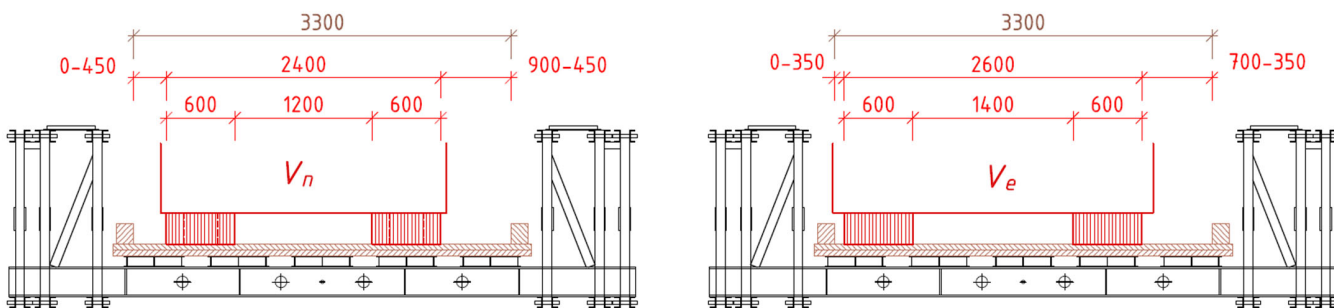


Figure 13. Positions of heavy vehicles within cross-section: V_n on the left, and V_e on the right.

The longitudinal placement of the load patterns was applied on the basis of moving load module considering their possible relief effects along the bridge. Hence, up to more than a hundred positions were analysed for each Bailey bridge model, depending on the BB system configuration.

The load factors were taken according to Eurocode 1 for traffic loads on bridges [19]. As this standard does not define separate dynamic load effects for road traffic load, dynamic factors ϕ calculated according to Equation (1) were considered in the analyses.

$$\phi = \frac{1}{0.95 - (1.4L_d)^{-0.6}} \leq 1.50 \quad (1)$$

In Equation (1), the abbreviation L_d represents the effective length in meters for each type of member. In the case of main girders and their components, the theoretical span can be taken into account. Thus, the dynamic factor applied to main girders internal forces varied from the value $\phi = 1.17$ in the case of longest analysed span with the length of 36.576 m, up to $\phi = 1.30$ in the case of span 12.196 m long. Similarly, the dynamic factors $\phi = 1.48$ for inclined struts (rakers) and $\phi = 1.50$ for all other members of BB superstructure were considered.

3.3. Stability Analysis

For the estimation of the resistance of top chord of the main girders, the out-of-plane buckling phenomena had to be carefully estimated. Except for the influences connected to traffic and corrosion damages [23], cases of collapsed Bailey bridges confirmed buckling instability as one of the most important failure modes of the structure [24]. Thus, attention was paid to the correct stability estimation of compression chords of the truss panels. The elastic analysis is suitable for the main girder behaviour, as failure mode of elastic buckling is occurring [25].

In order to identify the deformation ability of the pin joint in an out of plane direction, an in situ verification was executed (Figure 14). It was found that the tolerances in the pin joint permit horizontal displacement of the joint from the straight direction up to 55–60 mm in the case of two adjacent panels. Of course, such values are unrealistic on the construction site, but they indicate that the pin joint of the panels can be considered hinged even for horizontal moments. Therefore, the pin joints of panels were modelled as hinged joints in both horizontal and vertical directions.

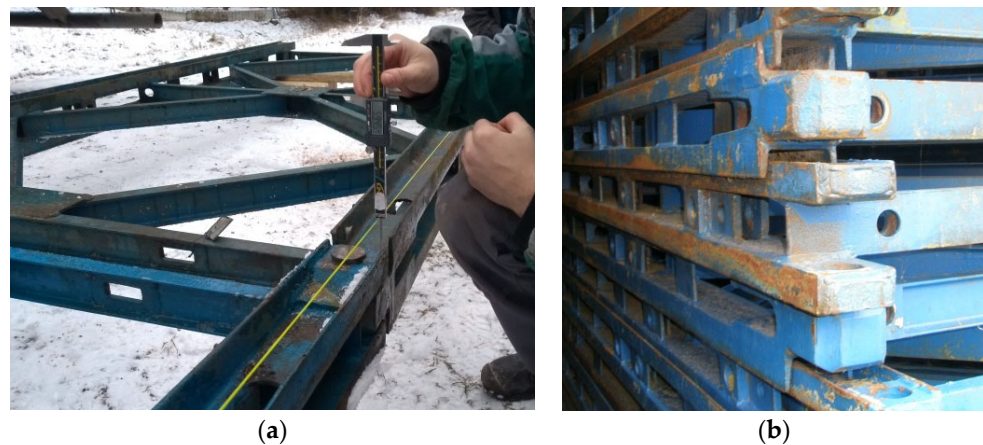


Figure 14. In situ verification of pin joint dimensions and its deformation capacity in horizontal direction: (a) measurement of horizontal deformation capacity of the joint; and (b) stored Bailey bridge panels.

The results of the elastic buckling analysis are usually expressed by the shapes of buckling modes (Figure 15), which are quantified by the critical buckling load factor α_{cr} applied in order to reach the elastic global instability.

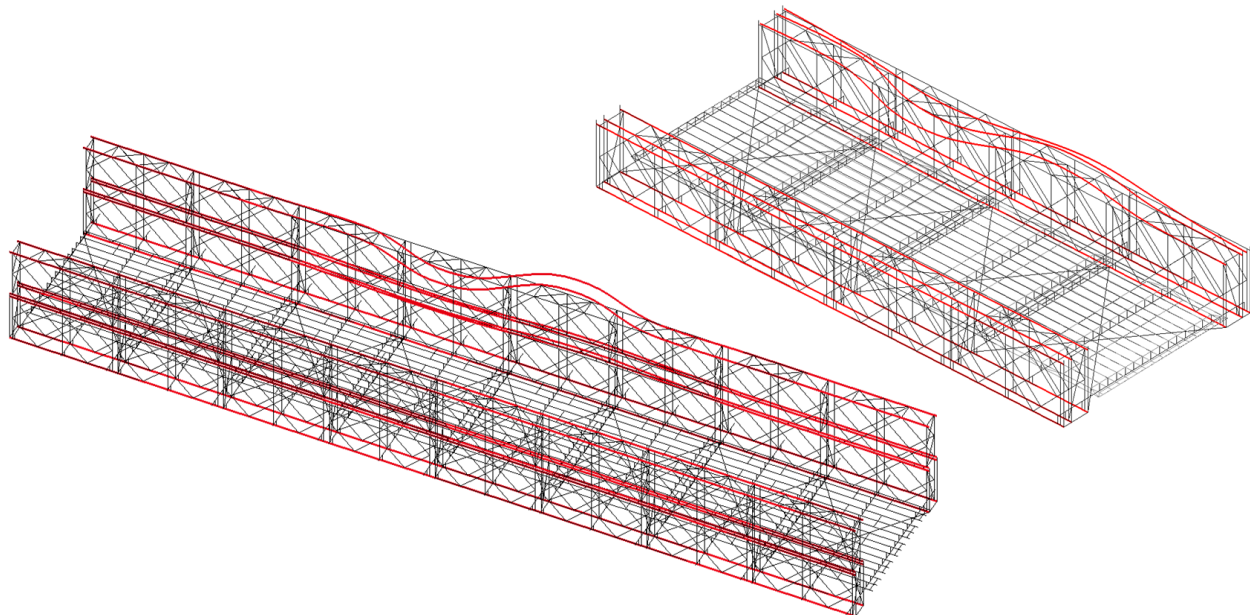


Figure 15. Examples of buckling modes of top chords in the case of BB composed as TS-12 (top right) and DD-24 (bottom left).

Thus, the critical buckling load factor α_{cr} represents an amplifier by which the design load would have to be increased to cause elastic instability [16]. Table 2 summarizes critical buckling load factors $\alpha_{cr,z}$ for all alternatives of Bailey bridges analysed in the study as

obtained for design load combinations. Based on the Euler's critical force, the buckling length $L_{cr,z}$ for out-of-plane buckling can be calculated according to the following equation:

$$L_{cr,z} = \pi \sqrt{\frac{EI_z}{\alpha_{cr,z} N_{Ed}}} \quad (2)$$

where E is modulus of elasticity of steel, I_z represents quadratic moment of the cross-sectional area of top chord (about the vertical axis), $\alpha_{cr,z}$ is the critical buckling load factor to reach the out-of-plane elastic global instability of top chords, and N_{Ed} is the design value of compressive force in a top chord member.

Table 2. Buckling parameters of out-of-plane buckling of the top chords.

Traffic Load in Combinations		V_n		V_e		
BB Arrangement	$\alpha_{cr,z}$ [—]	$N_{cr,z}$ [kN]	$L_{cr,z}$ [m]	$\alpha_{cr,z}$ [—]	$N_{cr,z}$ [kN]	$L_{cr,z}$ [m]
TS-12	7.53	4021	2.05	6.62	3743	2.12
TS-18	5.73	3182	2.30	5.65	3128	2.32
TS-21	4.79	2741	2.48	5.27	2967	2.38
DD-24	4.93	2925	2.40	5.22	3149	2.32
DD-27	4.83	2936	2.40	5.13	3088	2.34
TD-33	4.47	2695	2.50	4.90	2952	2.39
TD-36	4.38	2661	2.52	4.84	2928	2.40

Based on presented results it can be concluded that the main girders are not prone to out-of-plane instability. As the value of critical buckling load factor α_{cr} is between 3.0 and 10.0 in all cases, second order effects can be included into verification process indirectly, for example by the 'equivalent column method', [16]. Usually, if the value of α_{cr} is smaller than 3.0, a geometrical nonlinear analysis with imperfections included is required. Such an analysis is very time consuming in the case of a numerical model with large number of elements [13].

Moreover, from the values of derived critical buckling lengths $L_{cr,z}$, it is clear that the buckling lengths seem to be smaller than panel length, as they reach values from 2.05 to 2.50 m in the presented numerical analyses. Therefore, provided that all bracings (both bracing frames and sway bracings), rakers and all mutual connections are feasible in accordance with BB documentation, there will be probably no problems with stability of top chords, and a well-known equivalent column method can be utilized.

The statements concerning critical buckling load factor α_{cr} are also valid for the traffic loads smaller than load-carrying capacities of chords under compression, presented in the following sections, since data in Table 2 were obtained iteratively for ultimate value of compressive buckling resistance in the critical element of top chord, individually for each variant of BB structure.

4. Load-Carrying Capacity

As the probabilistic approach would be quite inefficient, [26], the semi-probabilistic engineering approach covered by Eurocode 3 was applied in this research [16,27]. All relevant verifications of cross-sections and members were performed. The possibility of local yielding was allowed only in cross-sections of class 1 and 2. In accordance to tests performed in [28], the cross-sections of BB members are able to resist such local yielding stresses in the case of ultimate loading.

The normal or exclusive load-carrying capacity V_n or V_e ($V_{n(e)}$) can be calculated according to the Equation (3), which is equivalent to equations according to regulations used in other countries [22,29]:

$$V_{n(e)} = \left[\left(R_d - \sum_{i=1}^{n-1} E_{rs,d,i} \right) / E_{Vn(e),d,REP} \right] \cdot V_{n(e),REP} \quad (3)$$

where: R_d is the design value of the resistance of the cross-section or bridge member; $E_{Vn(e),d,REP}$ is the value of static quantity due to effects of variable load model defined in Figure 11 or Figure 12, respectively, but only those parts of them, which depend on value of $V_{n,REP}$ or $V_{e,REP}$ (i.e., without uniformly distributed load 2.5 kN/m^2 in the case on normal load-carrying capacity); $\sum_{i=1}^{n-1} E_{rs,d,i}$ are the design, combination or group values of the effects of other (the rest) loads acting, including those parts of the variable road load model independent of value of $V_{n,REP}$ or $V_{e,REP}$, respectively; finally designation $V_{n(e),REP}$ express representative values of weight of vehicles implemented into global analysis by which static entities $E_{Vn(e),d,REP}$ were produced.

In order to apply the principle of proportionality and to simplify the calculation process, the relative values for load-carrying capacities were considered in a linear global analysis. Thus, load schemes were modelled in FEM analysis with its specified so-called ‘representative’ values and relative load-carrying capacity Z were calculated according to Equation (4). Namely, the representative weight of the modelled ‘normal’ vehicle was set to $V_{n,REP} = 32 \text{ tons}$ and implemented into all particular load cases, while for the representative weight of ‘exclusive’ vehicle, the value of $V_{e,REP} = 40 \text{ tons}$ was used. Thus, those values correspond to relative load-carrying capacity $Z = 1.0$. The basic formulae for obtaining relative load-carrying capacity Z can be then written as:

$$Z_{n(e)} = \left(R_d - \sum_{i=1}^{n-1} E_{rs,d,i} \right) / E_{Vn(e),d,REP} \quad (4)$$

where all symbols were defined under Equation (3).

The use of relative values of load-carrying capacity Z is common for railway bridges, where it represents a relative ratio to the effects produced by railway traffic load models [30]. Anyway, for the public roads, the values of maximum permissible weight of a vehicle passing the bridge in tons are commonly utilised, as they can be controlled and defined by traffic signs. As relative value Z is a function of specified value of the modelled representative vehicles $V_{n,REP}$ or $V_{e,REP}$, respectively, the load carrying capacity can be then calculated according to Equations (5) and (6), as follows:

$$V_n = Z_n \cdot V_{n,REP} = Z_n \cdot 32 \text{ t} \quad (5)$$

$$V_e = Z_e \cdot V_{e,REP} = Z_e \cdot 40 \text{ t} \quad (6)$$

Combinations of internal forces in a critical cross-section have been taken into account. Therefore, the iteration process had to be utilized to obtain ultimate values of unknown relative values Z_n and Z_e , or final load-carrying capacities of verified elements V_n and V_e , respectively. As calculations of load-carrying capacity have to be done for many of verification procedures according to Eurocode 1 [16,19], the whole procedure was programmed. If stability was the issue, the verification of buckling resistances of members under compression and/or lateral-torsional buckling of members under bending moment were executed repeatedly as well.

More information concerning the relative load-carrying capacity estimation, including techniques for how the relative load-carrying capacity can be analytically derived for several verification formulas in accordance with Eurocode 1 [16,19], can be found in [30–33].

When determining the load-carrying capacity of individual Bailey bridge elements, it was assumed that the welded connections of the members are designed for the overall axial capacity of corresponding element. Thus, the load-carrying capacity in the study is not limited by the load-carrying capacity of the connections, but always by a specific member resistance given in tables in the following section. Serviceability limit states (especially deflection) were not assessed.

5. Results and Discussion

The following tables bring an overview of the load-carrying capacities of the main parts of the Bailey bridge system. The values are presented in all cases in tons.

5.1. Main Girders

Load-carrying capacities of the main girders are given in Tables 3 and 4. Grey highlighted are the values which are less than 28 tons in the case of normal load-carrying capacity V_n and 40 tons in the case of exclusive load-carrying capacity V_e , respectively. In addition, the values of V_n smaller than 22 tons and of V_e smaller than 32 tons are underlined to point out that they represent values very far from the required level defined at the beginning of the study. Thus, the applicability of main girders is clear from both tables.

Table 3 presents the normal load-carrying capacities of members of Bailey bridge system. It can be seen that for the most cases the bottom chords and compressed truss elements of the BB panels (diagonals and verticals) do not meet the requirements for the assumed normal load-carrying capacity ($V_n = 28$ tons). Despite of that, these results do not lead to the conclusion that the BB system cannot be utilized for such variants and spans at all. These BB system configurations can still be utilized; however, the weight of the vehicles allowed to cross the bridge has to be limited to given levels. The similar conclusions can be derived for exclusive load-carrying capacity according to Table 4.

In addition, the tables show the elements of the main girders that would need to be strengthened and thus ensure the use of the individual BB truss panels to the required or even higher level of load-carrying capacity.

As a real example, the solution to satisfy demands on exclusive load-carrying capacity up to 40 tons for Bailey bridge TS-12 is shown in Figure 16. As a result of static analysis came the necessity to avoid the BB panels with diagonals and verticals made of I-profiles due to their insufficient capacity in comparison with the panels where U-profiles were used for diagonals and verticals. Anyway, this requirement is inevitable only for the panels near supports (first and last panels within span), and moreover only for the inner and the middle main girders' panels. Such a requirement arises from smaller compression capacity of I-sections used for diagonals and verticals due to its lower buckling resistance in comparison with common U-profiles. Thus, for the remaining 16 out of a total 24 panels, any panels can be applied.

Table 3. Normal load-carrying capacities of main girders parts.

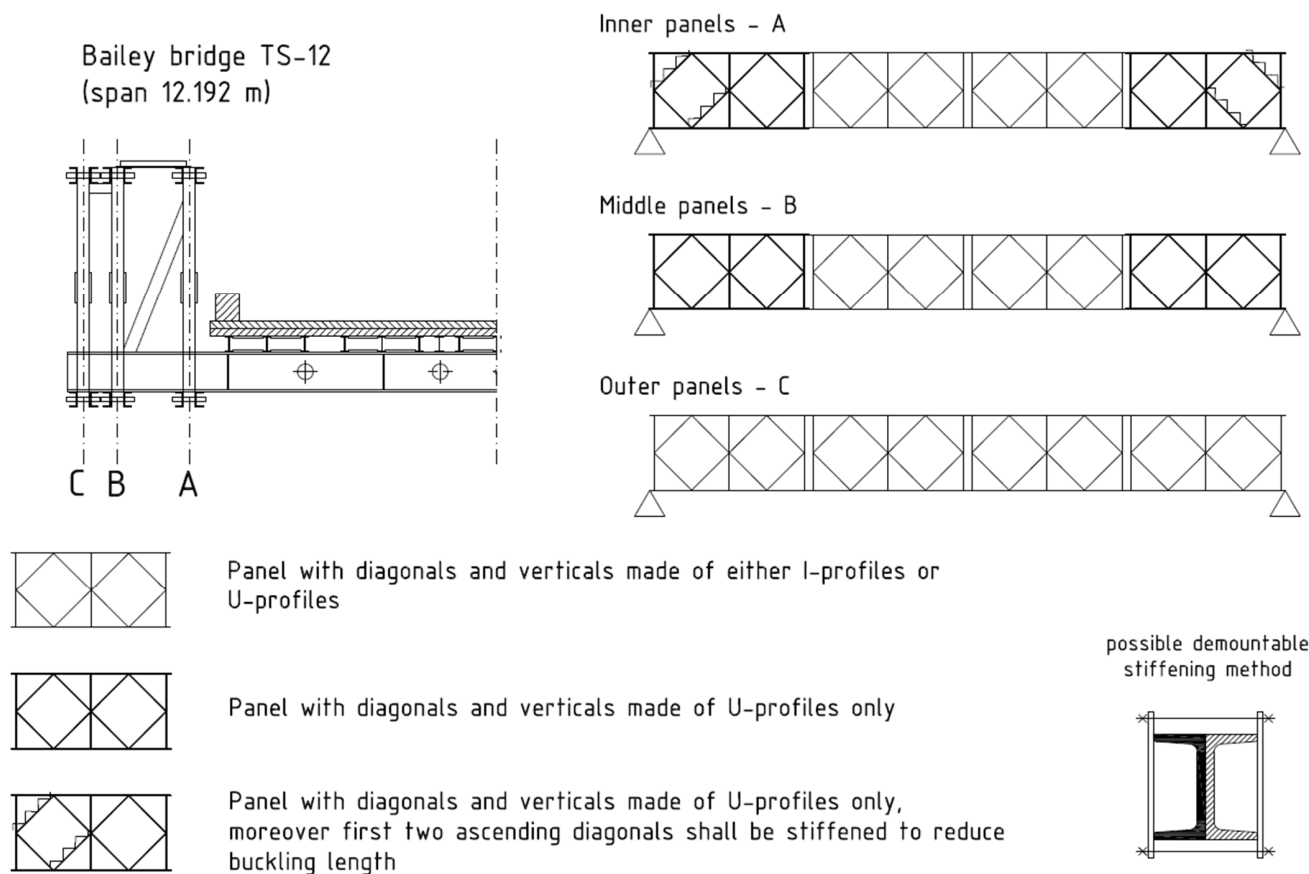
Normal Load-Carrying Capacity [tons]	Configuration	TS-12	TS-18	TS-21	DD-24	DD-27	TD-33	TD-36
		Span Length [m]	12.192	18.288	21.336	24.384	27.432	33.528
	Predominant Stress	V_n	V_n	V_n	V_n	V_n	V_n	V_n
Chords	T + B (bottom)	21.1	22.9	18.4	22.1	16.3	17.7	15.6
	C (top)	54.8	38.0	30.0	41.2	30.9	27.5	20.4
Diagonals U	C	22.6	19.8	18.6	23.0	21.5	22.3	21.3
	T	39.1	42.1	40.1	44.0	42.4	43.5	42.7
Diagonals I	C	18.9	16.5	15.4	19.0	17.7	18.4	17.7
	T	45.8	45.0	43.0	47.1	45.2	46.7	45.6
Verticals U	C	30.1	26.8	25.9	27.7	25.0	24.8	25.0
	T	40.0	40.3	38.6	40.0	40.4	41.0	41.2
Verticals I	C	25.4	22.4	21.7	22.7	20.1	20.6	19.9
	T	42.3	42.5	42.2	43.6	44.1	44.6	44.9
Rakers	C	31.3	34.3	31.3	37.2	37.2	40.7	43.5
End posts	T	92.6	91.4	67.3	95.2	79.4	83.6	80.0
Sway braces	C	65.3	62.4	62.4	46.5	44.5	53.5	52.2
Pin joint	T	66.1	58.1	54.0	61.0	55.5	51.7	47.0
Chord bolts	S + B	92.4	64.1	51.4	58.7	47.6	44.5	35.2
	S + T				66.7	61.8	63.7	60.9

Nomenclature for as yet undefined predominant stress: T—tension; C—compression; B—bending; S—shear.

Table 4. Exclusive load-carrying capacities of main girders parts.

Exclusive Load-Carrying Capacity [tons]	Configuration	TS-12	TS-18	TS-21	DD-24	DD-27	TD-33	TD-36
		Span Length [m]	12.192	18.288	21.336	24.384	27.432	33.528
Chords	Predominant Stress	V_e	V_e	V_e	V_e	V_e	V_e	V_e
	T + B (bottom)	53.1	47.7	37.0	45.7	40.0	46.9	40.0
Diagonals U	C (top)	76.2	50.6	42.0	59.8	51.4	55.2	47.8
	C	33.2	34.1	33.4	46.5	45.9	47.4	47.0
Diagonals I	T	56.9	64.0	60.8	78.5	78.2	81.2	80.9
	C	28.9	29.9	29.3	40.5	39.8	41.1	40.6
Verticals U	T	64.6	66.7	65.3	82.4	82.2	85.2	85.0
	C	46.2	44.7	45.1	49.2	48.8	51.8	52.1
Verticals I	T	62.5	64.2	61.0	91.0	92.0	93.2	93.8
	C	40.6	39.0	38.9	41.9	41.5	45.2	44.6
Rakers	T	73.2	75.3	71.3	98.1	99.1	100.4	101.1
	C	42.1	30.7	30.7	51.2	51.3	51.8	56.2
End posts	C	75.8	76.3	74.6	68.9	70.1	77.0	76.5
Sway braces	T	80.3	71.2	67.2	87.6	80.9	79.6	76.7
Pin joint	S + B	68.8	72.3	73.4	74.4	75.1	76.2	76.7
Chord bolts	S + T				113.2	109.8	115.4	114.1

Nomenclature for as yet undefined predominant stress: T—tension; C—compression; B—bending; S—shear.

**Figure 16.** Example of enhancement of load-carrying capacity by arrangement of panels.

This example confirms that in the case of shorter spans of the three-girder alternatives of the Bailey bridge, the two inner main girders (i.e., the inner and the middle ones) are much more loaded than the outer one. The analysis revealed an additional requirement to increase the buckling resistance of first two compressed diagonals of the inner girder. As the load-carrying capacity based on resistance of the cross-section was sufficient enough, a

simple enhancement of stiffness of these diagonals for in-plane buckling could be suggested, as shown in Figure 16.

5.2. Deck Members

The determined load-carrying capacities of stringers and cross beams are given in Tables 5–8. The normal and exclusive load-carrying capacities are presented together with the maximum permissible weight per axle. Similar to the above results reported for main girders, data valid for deck members in the tables below are grey highlighted when the values of normal and exclusive load-carrying capacities are $V_n < 28$ tons and $V_e < 40$ tons, respectively. As in Section 5.1, the underlined values are those less than 22 tons for the normal load-carrying capacity and less than 32 tons in the case of the exclusive load-carrying capacity. Accordingly, the limit values for highlighting or underlining the values applicable to the maximum permissible weight per axle were considered to be 12 tons, and 10 tons respectively.

Table 5. Stringer load-carrying capacity for panels with 2 cross beams.

Stringers with Spans of 1608 + 1440 mm (2 Cross Beams within Each Panel)							
Load-Carrying Capacity [tons]		Normal LCC V_n		Exclusive LCC V_e		Axle Weight	
		Standard Deck	Stiffer Deck	Standard Deck	Stiffer Deck	Standard Deck	Stiffer Deck
original	mid-span	10.0	11.9	31.7	38.1	7.5	8.9
	mid-support	12.8	15.0	38.3	42.7	9.6	10.7
IPN100	mid-span	13.1	15.5	41.2	49.1	9.8	11.6
	mid-support	16.9	19.9	49.7	55.9	12.4	14.0
IPN120	mid-span	20.8	24.4	64.3	76.2	15.6	18.3
	mid-support	26.2	31.2	76.3	86.2	19.1	21.5

Nomenclature: LCC—Load-carrying capacity.

Table 6. Stringer load-carrying capacity for panels with 3 cross beams.

Stringers with Spans of 1440 + 1290 + 318 mm (3 Cross Beams within Each Panel)							
Load-Carrying Capacity [tons]		Normal LCC V_n		Exclusive LCC V_e		Axle Weight	
		Standard Deck	Stiffer Deck	Standard Deck	Stiffer Deck	Standard Deck	Stiffer Deck
original	mid-span	12.6	12.4	37.2	38.4	9.3	9.3
	mid-support	18.1	17.6	51.0	53.8	12.8	13.2
IPN100	mid-span	16.6	16.3	48.2	49.6	12.1	12.3
	mid-support	24.6	24.2	66.7	63.0	16.7	15.8
IPN120	mid-span	26.5	26.2	75.3	77.6	18.8	19.4
	mid-support	39.7	39.7	99.4	90.5	24.9	22.6

Table 7. Cross beam load-carrying capacity when three cross beams are used per panel.

Three Cross Beams within Each Panel (Stringers with Spans of 1440 + 1290 + 318 mm)				
Load-Carrying Capacity [tons]	Cross beam	Normal LCC		Axle Weight
		V_n	V_e	
DS	DS	28.3	57.1	14.3
	TS	29.8	56.1	14.0
	DD	28.2	56.7	14.2
	TD	28.9	55.6	13.9

Table 8. Cross beam load-carrying capacity when two cross beams are used per panel.

Two Cross Beams within Each Panel (Stringers with Spans of 1608 and 1440 mm)				
Load-Carrying Capacity [tons]	Cross beam	Normal LCC		Axle Weight
		V_n	V_e	
DS	DS	21.5	40.0	10.0
	TS	24.5	47.3	11.8

5.2.1. Stringers

The load-carrying capacities of stringers for two alternatives of the timber deck cover are presented. The tables also differentiate between locations of the most stressed cross-section along the member, at mid-span and mid-support specifically.

It is understandable, that the load-carrying capacity of the stringers is basically not dependent on the configuration of main girders.

Table 5 represents the structural configuration of the deck system with two cross beams within each panel, which determines the spans of the stringers of 1608 + 1440 mm. Load-carrying capacities for deck system with three cross beams for each panel with spans of stringers of 1400 + 1290 + 318 mm are presented in Table 6.

It is clear that the resistance of the mid-span cross-section of stringers appears to be crucial. It can also be seen that the stringers made of the original I-type cross-section (currently RSJ 102/44/7) provide a very low load-carrying capacity, which does not even reach the value of 10 tons for the maximum permissible weight per axle, even when the stiffer timber deck is realized.

The utilization of hot-rolled IPN100 profiles enhances the exclusive load-carrying capacity of the stringers to the desired numbers. Moreover, this configuration is able to satisfy the required values of exclusive load-carrying capacities even with the usage of a standard deck and provides also the values of maximum permissible weight per axle sufficient for most lorries. However, to obtain an acceptable values of normal load-carrying capacity four cross beams per panel would probably be needed.

The alternative with hot-rolled IPN120 profiles satisfy all requirements on load-carrying capacity with sufficient reserves. It is obvious, that they are able to carry higher loads than preceding alternatives. It is therefore appropriate to propose this solution especially for temporary bridges with the expected longer-term use not only in terms of load-carrying capacity, but also the durability of the bridge deck.

5.2.2. Cross Beams

The load-carrying capacity of cross beams presented in Table 7 relates to the configuration of three cross beams per panel, with the mutual distances of 1400 + 1290 + 318 mm. The typical 10-inch I-section (currently RSJ 254/114/37) with 102 mm openings in the web was verified. The values are specified for both single and double-story systems with both double and triple-truss arrangement. The configuration of the timber deck system has only a small influence on the load-carrying capacity of cross beam. Additionally, the load-carrying capacity of cross beams is only partially dependent on the span of the main girders. It is due to the fact that the cross beams are additionally loaded by stresses resulting from their function as part of the transverse half-frames ensuring the stability of the main girders. However, the differences among the BB models are small, and are mostly influenced by the rotational stiffness of the connection to the main girders. The differences, although small, are therefore caused by the presence of two or three transom clamps, depending on whether the analysed BB has double and triple-truss arrangement.

According to Table 7, it can be stated that if three original cross beams per panel are used, they sufficiently satisfy the requirements for exclusive load-carrying capacity introduced. Moreover, the cross beams are also able to meet requirements for acceptable normal load-carrying capacity, i.e., the conventional lorries with weight up to 28 tons can cross the bridge without any traffic restrictions.

Table 8 presents the reduction in load-carrying capacity of cross beams if only two cross beams per panel of BB are used with the mutual distances of 1608 and 1440 mm. This seems to be not very reasonable solution. The exclusive load-carrying capacity is around the required limit, but the value of normal load-carrying capacity has decreased, especially in case of double-truss BB is this reduction more severe.

6. Conclusions

In this paper, the study on load-carrying capacity of Bailey bridges is presented. Except for situations after natural disasters, the applications of BB as temporary construction arose with expansion of building industry. In addition, there are a few examples of the Bailey bridge used as a “semi-term” or even “long-term” bridge only in the region of Slovakia and Czechia. As demands on utilisation of Bailey bridges for civil purposes are growing, a brief overview of options of this bridge system is very helpful.

Values of the load carrying capacities given in Tables 3–8 provide a very good overview of the applicability of the individual structural arrangements of the main girder or bridge deck analysed. However, what is just as valuable, the tables show the possibility of utilisation of each element or, on the other hand, the necessity of its strengthening to enhance its load-carrying capacity to not be the limiting element within the structure.

The applied load schemes have been proven for decades and provide a realistic picture of the possible permissible weight of vehicle passing the bridge both in normal or exclusive traffic situation. The reasons why it was decided to use the schemes according to Figures 11 and 12 are clarified in Section 3.2. It should be noted that a single-line narrow bridge is the issue, most often used on a construction site or on a local road network. Anyway, next study is planned, where results of the research given in [20,21] and therein proposed scheme will be utilised. Some comparison can be then made to see the differences in obtained permissible weight of vehicles.

On the basis of presented results in the previous chapter it is possible to decide on deployment of specific configuration of main girder panels and deck members for BB system for various spans. The proposed load-carrying capacities are on the safe side as the same reliability levels that are prescribed by Eurocodes for newly designed structures are assumed. Thus, actual load-carrying capacities could be increased for the temporary bridges. Moreover, modern methodologies for the evaluation of bridge structures for their expected remaining life-time can be used [22,29]. Then, modification of reliability indexes for the evaluation of existing bridges would lead into reduction of the partial reliability factors. The basic concept of how the reliability levels can be transformed into the design values of the material properties and load effects could be found in the paper [34].

However, all abovementioned data, recommendations and conclusions assume a faultless condition of the bridge structure. Such a condition is unrealistic, also due to the underestimated maintenance, which supports the conditions for rapid degradation in any existing bridge structure [35]. In real applications, it is therefore necessary to take into account the possible damage of essential components [36]. In addition to frequent corrosion attacks, especially of deck elements, imperfections caused by impacts or unprofessional handling of bridge parts often occur. These, as well as any other failures, must be taken into account when determining the resistance and consequent load-carrying capacity of individual cross-sections and members [37]. However, in the cases where failures can also have impact on the redistribution of internal forces, they need to be implemented into the global design analysis as well.

Accordingly, the utilization of this study requires experience both with application and maintenance of the Bailey bridge system, and also a broader perspective to account its hidden reserves or possible defects.

Author Contributions: Conceptualization, J.O. and V.N.; methodology, J.O.; software, J.P. and M.F.; validation, J.O. and J.P.; formal analysis, J.P. and M.F.; investigation J.O. and J.P.; resources, J.O. and V.N.; data curation, J.P and M.F.; writing—original draft preparation, J.O.; writing—review and editing, J.P.; visualization, J.P.; supervision, J.O. and V.N.; project administration, J.P.; funding acquisition, J.O. All authors have read and agreed to the published version of the manuscript.

Funding: This research was supported by Research Project No. 1/0630/21 of the Slovak Grant Agency and by the project of Operational Programme Interreg V-A Slovak Republic–Czech Republic No. 304011Y277 (the project is co-funding by European Regional Development Fund).

Institutional Review Board Statement: Not applicable.

Informed Consent Statement: Not applicable.

Data Availability Statement: Data sharing not applicable.

Conflicts of Interest: The authors declare no conflict of interest.

References

1. Benda, M.; Manas, P. Temporary Bridges Used in the Czech Republic. In Proceedings of the International Conference on Military Technologies (ICMT), Brno, Czech Republic, 31 May–2 June 2017; pp. 252–256.
2. Ingham, B. Temporary bridging: Principles of design and construction. In *Temporary Works*, 2nd ed.; Pallett, P.F., Filip, R., Eds.; Ice Publishing: London, UK, 2018; Chapter 19; pp. 251–262.
3. *Field Manual: Bailey Bridge*; FM 5-277; Headquarters Department of the Army: Washington, DC, USA, 1986. Available online: <http://www.bits.de/NRANEU/others/amd-us-archive/fm5-277%2886%29.pdf> (accessed on 20 February 2022).
4. Jackson, G.B. *The Bailey Bridge*; New Zealand Engineering: Wellington, New Zealand, 1949; p. 1003.
5. Roberts, L.D. The Bailey: The Amazing, All-Purpose Bridge. In *Builders and Fighters: U.S. Army Engineers in World War II*, 1st ed.; Fowle, B.W., Ed.; United States Army Corps of Engineers: Fort Belvoir, VA, USA, 1992; pp. 181–193.
6. Bujňák, J.; Vičan, J.; Odrobiňák, J. Proof Load Tests and FEM Model as a Tools for Verification of Real Bridge Behaviour. In Proceedings of the 8th International Conference on Short & Medium Span Bridges, Niagara Falls, ON, Canada, 3–6 August 2010; p. 148/1–10.
7. STANAG 2021; Military Load Classification of Bridges, Ferries, Rafts and Vehicles. NATO: Brussels, Belgium, 2017.
8. Yi, P.; Vaghela, G.; Buckland, A. Condition Assessment and Load Rating of Arced Bailey Bridge. In Proceedings of the 9th Austroads Bridge Conference, Sydney, NSW, Australia, 22–24 October 2014; ARRB: Port Melbourne, Australia, 2014.
9. Khounsida, T.; Nishikawa, T.; Nakamura, S.; Okumatsu, T.; Thepvongsa, K. Study on Static and Dynamic Behavior of Bailey Bridge. In Proceedings of the 2019 World Congress on Advances in Structural Engineering and Mechanics (ASEM19), Jeju Island, Korea, 17–21 September 2019.
10. Lee, J.W.; Yoo, S.H.; Kim, I.S.; Kim, T.Y.; Choi, H.H.; Yoon, W.S.; Kim, Y.C. A study on the Analysis for the Strength of Bailey Panel Bridge. *J. Korea Inst. Mil. Sci. Technol.* **2011**, *14*, 15–21. [[CrossRef](#)]
11. SCIA Engineer. *Reference Guide*; Nemetschek Group: Hasselt, Belgium, 2013.
12. Jindra, D.; Kala, Z.; Kala, J. A comparison of FE Analysis of Columns Utilizing Two Stress-strain Material Relations and Two Different Solvers: ANSYS vs SCIA Engineer. In Proceedings of the International Conference on Computational Plasticity, Barcelona, Spain, 7–9 September 2021; 9 September 2021.
13. Odrobiňák, J.; Farbák, M.; Chromčák, J.; Kortiš, J.; Gocál, J. Real Geometrical Imperfection of Bow-String Arches—Measurement and Global Analysis. *Appl. Sci.* **2020**, *10*, 4530. [[CrossRef](#)]
14. Parivallal, S.; Narayanan, T.; Ravisankar, K.; Kesavan, K.; Maji, S. Instrumentation and Response Measurement of a Double-Lane Bailey Bridge During Load Test. *Strain* **2005**, *41*, 25–30. [[CrossRef](#)]
15. Chen, W.Z.; Yan, B.C.; Liu, X.; Jiang, Y.D. Research on the Finite Element Simulation of and Updating Method for Old Riveted Truss Bridges. *Stahlbau* **2012**, *81*, 419–425. [[CrossRef](#)]
16. EN 1993-1-1; Eurocode 3: Design of Steel Structures—Part 1-1: General Rules and Rules for Buildings. CEN: Brussels, Belgium, 2005.
17. EN 1991-4; Eurocode 1: Actions on Structures—Part 1-4: General Actions—Wind Actions. CEN: Brussels, Belgium, 2005.
18. Leahy, C.; OBrien, E.; O'Connor, A. The Effect of Traffic Growth on Characteristic Bridge Load Effects. *Transp. Res. Procedia* **2016**, *14*, 3990–3999. [[CrossRef](#)]
19. EN 1991-2; Eurocode 1: Actions on Structures—Part 2: Traffic Loads on Bridges. CEN: Brussels, Belgium, 2006.
20. Vičan, J.; Odrobiňák, J.; Gocál, J. Determination of Road Bridge Load-Carrying Capacity. *Civ. Environ. Eng.* **2021**, *17*, 286–297. [[CrossRef](#)]
21. Gocál, J.; Odrobiňák, J.; Vičan, J. On the Load-Carrying Capacity Produced by Different Load Models for Road Bridges. *IOP Conf. Ser. MSE Civ. Eng. Conf. Košice 2022*, *10*, accepted, in press.
22. Skokandić, D.; Ivanković, A.M.; Znidarić, A.; Srbic, M. Modelling of traffic load effects in the assessment of existing road bridges. *Gradevinar* **2019**, *71*, 1153–1165.
23. Kamruzzaman, M.; Haque, M.R. Assessment of Dead Load Deflection of Bailey Bridge. In Proceedings of the IABSE-JSCE Joint Conference on Advances in Bridge Engineering-IV, Dhaka, Bangladesh, 26–27 August 2020; pp. 306–310.
24. Kaushik, H.B.; Talukdar, S. Structural Assasment of a Collapsed Bailey Bridge over Tuirini River on NH-150 in Aizawl, Mizoram. Report Submitted to Deputy Commissioner, Aizawl, Mizoram. 2018. Available online: <https://pwd.mizoram.gov.in/uploads/attachments/0b3455e113ace8c59ea54cc252dbf032/posts-67-structural-assessment-of-collapsed-bailey-bridge-over-tuirini-river-1.pdf> (accessed on 20 February 2022).
25. King, W.S.; Duan, L. Experimental Investigations of Bailey Bridges. *J. Bridge Eng.* **2003**, *8*, 334–339. [[CrossRef](#)]
26. Kala, Z.; Seitl, S.; Krejsa, M.; Omishore, A. Reliability Assessment of Steel Bridges Based on Experimental Research. In Proceedings of the International Conference on Numerical Analysis and Applied Mathematics (ICNAAM), Rhodes, Greece, 13–18 September 2018. published 2019.
27. EN 1993-2; Eurocode 3: Design of Steel Structures—Part 2: Steel Bridges. CEN: Brussels, Belgium, 2006.

28. King, W.S.; Wu, S.M.; Duan, L. Laboratory Load Tests and Analysis of Bailey Bridge Segments. *J. Bridge Eng.* **2013**, *18*, 957–968. [[CrossRef](#)]
29. Paeglis, A.; Paeglitis, A. Simple Classification Method for the Bridge Capacity Rating. *Constr. Sci. Sci. J. Riga Tech. Univ.* **2010**, *11*, 44–50.
30. Vičan, J.; Gocál, J.; Odrobiňák, J.; Koteš, P. Existing steel railway bridges evaluation. *Civ. Environ. Eng.* **2016**, *12*, 103–110. [[CrossRef](#)]
31. *UIC 70778-2; Recommendations for Determining the Carrying Capacity and Fatigue Risks of Existing Metallic Railway Bridges*; Aft. International Union of Railway: Paris, France, 2021; 77p.
32. Railways of the Slovak Republic. *General Technical Requirements: Determination of Load Carrying Capacity of Railway Bridges*; Railways of the Slovak Republic: Bratislava, Slovakia, 2015; 116p. (In Slovak)
33. *Regulation SŽ S5/1; Diagnostics, Load-Carrying Capacity and Pass Ability of Railway Bridges*. Czech Railway Administration: Prague, Czech Republic, 2021; 156p. (In Czech)
34. Koteš, P.; Vičan, J. Recommended Reliability Levels for the Evaluation of Existing Bridges According to Eurocodes. *Struct. Eng. Int.* **2013**, *23*, 411–417. [[CrossRef](#)]
35. Odrobiňák, J.; Hlinka, R. Degradation of Steel Footbridges with Neglected Inspection and Maintenance. *Procedia Eng.* **2016**, *156*, 304–311. [[CrossRef](#)]
36. Gocál, J.; Odrobiňák, J. On the Influence of Corrosion on the Load-Carrying Capacity of Old Riveted Bridges. *Materials* **2020**, *13*, 717. [[CrossRef](#)] [[PubMed](#)]
37. Macho, M.; Ryjacek, P.; Matos, J. Fatigue Life Analysis of Steel Riveted Rail Bridges Affected by Corrosion. *Struct. Eng. Int.* **2019**, *29*, 551–562. [[CrossRef](#)]